Electronic Supplementary Material (ESI) for Materials Horizons.

Self-Branched α–MnO_2/δ–MnO_2 Heterojunction Nanowires With Enhanced Pseudocapacitance

Changrong Zhu,[a,b] Lu Yang,[a] Joon Kyo Seo,[a] Xiao Zhang,[c] Shen Wang,[a] JaeWook Shin,[a] Dongliang Chao,[b] Hua Zhang,[c] Ying Shirley Meng,[a]* Hong Jin Fan[b]*

[a] *Department of NanoEngineering, University of California San Diego, La Jolla, California 92093-0448, USA*

[b] *School of Physical and Mathematical Sciences, Nanyang Technological University, 637371, Singapore*

[c] *Center for Programmable Materials, School of Materials Science and Engineering, Nanyang Technological University, 639798, Singapore*

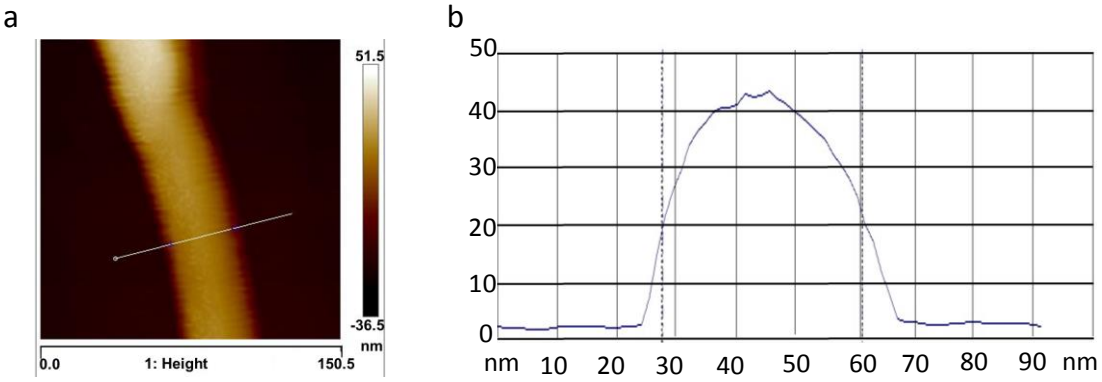

Figure S1. S1 AFM characterization of α-MnO_2 nanowires. a) Line profile and b) the height distribution of a single α-MnO_2 nanowire.

Table S1. Raman peak positions of pure α-, δ-, and Self-branched MnO_2

Sample	V_1	V_2	V_3	V_4	V_5	V_6	V_7
α-MnO_2 Nanowire	640	579	516	390	332	183	-
δ-MnO_2	647	577	492	403	290	-	143
Self-branched MnO_2	648	579	500	397	283	185	136

Raman fitting results analysis:

V_1: located at 640 ~ 650 cm^{-1}, can be assigned to the symmetric stretching vibration of [Mn-O] of MnO_6 octahedral;[1, 2]

V_2: located at 570 ~ 580 cm^{-1}, is attributed to [Mn-O] stretching along the chains of the MnO_2 framework.[1, 2]

V_3: located at 490 ~ 500 cm^{-1}, is due to the deformation mode of the metal–oxygen chain Mn–O–Mn in the [MnO_6] octahedral lattice.[3, 4]

V_4: located at 390 ~ 410 cm^{-1}, corresponds to the stretching mode of the [MnO_6] octahedra.[4]

V_5: located at 280 ~ 330 cm^{-1}, corresponds to infrared-active modes.[5]

V_6: located at 183 cm^{-1}, is assigned to the external vibration of translational motion of MnO_6 octahedral related to the tunnel cation.[2, 6]

V_7: located at 130-150 cm^{-1}, is assigned to the external vibration of translational motion of MnO_6 octahedral related to the water molecules in the MnO_2 layers.[2-4]

V_3~V_5: 280 ~ 500 cm^{-1}, those infrared-active modes could also be caused by the formation of the electrochemically irreversible low valence manganese oxides such as Mn_2O_3 and Mn_3O_4, and the dissolution of Mn species from the electrode or octahedra polymerization.[5]

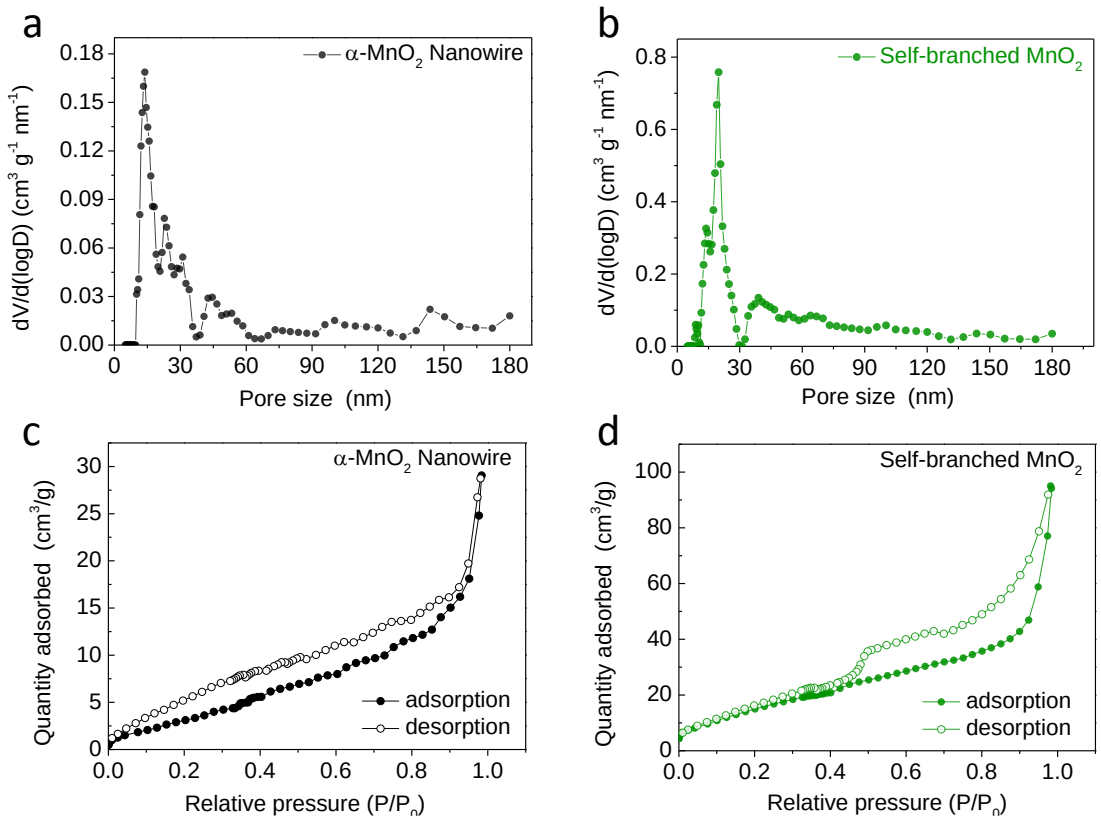

Figure S2. BET test of MnO_2 samples. Pore size distribution of a) α-MnO_2 nanowire and b) self-branched-MnO_2 nanostructure; N_2 Adsorption-desorption isotherms of c) α-MnO_2 nanowire and d) self-branched-MnO_2 nanostructure.

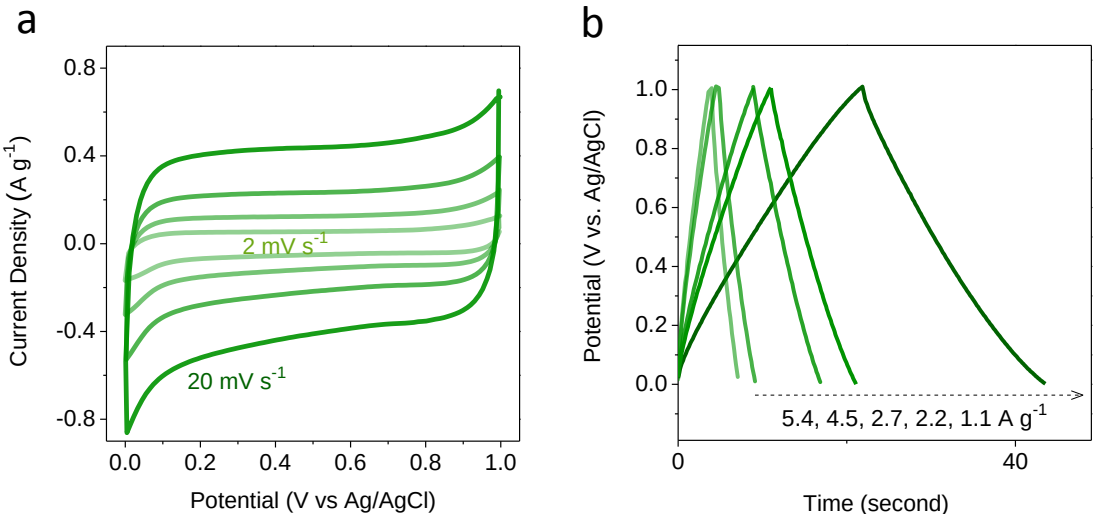

Figure S3. CV curves a) and charge-discharge curves b) of α-MnO_2 nanowire at different scan speed and current density.

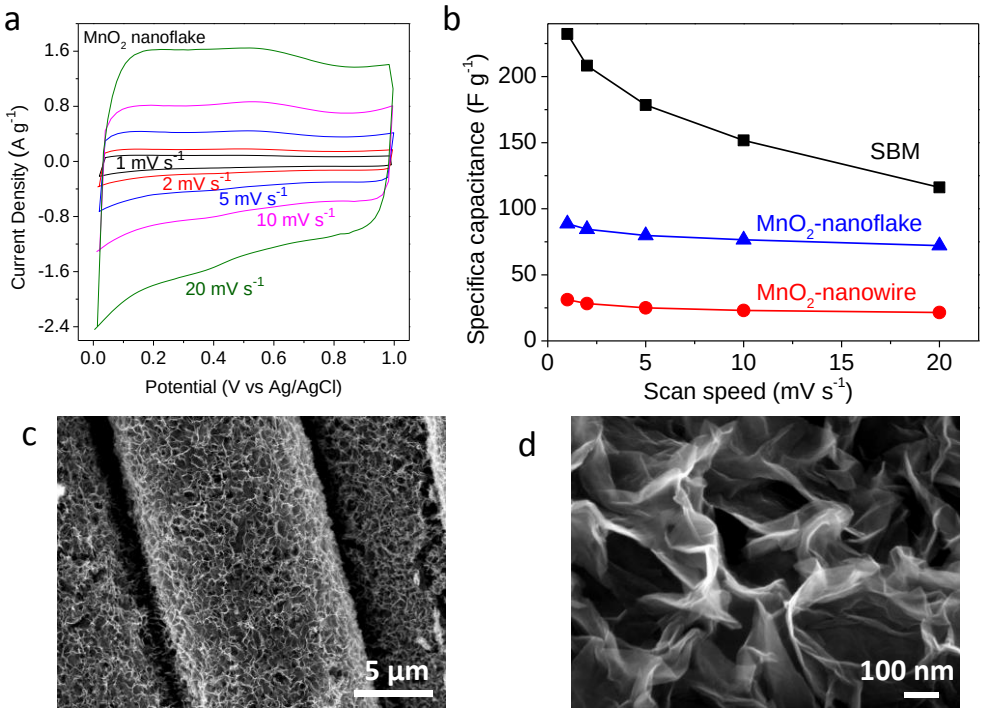

Figure S4. a) CV curves of δ-MnO_2 nanoflakes on carbon paper at different scan speeds; b) Comparison of the specific capacitance of the self-branch electrode, α-MnO_2 nanowire electrode, and δ-MnO_2 nanoflake electrode. (c and d) SEM images of different magnifications of the δ-MnO_2 nanoflakes on carbon fibers.

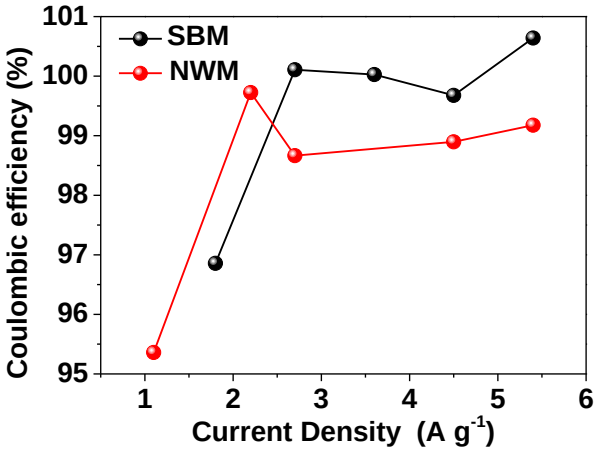

Figure S5. Coulombic efficiency at different current densities of α-MnO_2 nanowire (NWM) and self-branched-MnO_2 nanostructure (SBM) electrodes, as calculated from their galvanostatic charge/discharge curves using the equation $E = \frac{Q_{Discharge}}{Q_{Charge}}$.

Calculation of capacitance contribution

According to Dunn et. al.[7], we explain the calculation details of capacitance contribution differentiation based on the CV curves as follows.

First, the current against scan speed be expressed in the equation:

$$i = av^b \qquad (1)$$

where i is the measured current under certain voltage, v is the sweep rate, a and b are adjustable parameters. When b equals 1, the current is fully contributed by capacitive behavior; When b equals 0.5, the current is fully ion-diffusion controlled contribution. The b value can be obtained by plotting current and sweep rate in logarithm, namely, the gradient of linear plots.

$$\log i = b \log v + \log a \qquad (2)$$

In reality, the current can originate from both aforementioned contributions. Therefore, the b value can vary between 0.5 and 1. Taking that into consideration, we can rewrite Equation (1) so that the current is a sum of two parts: capacitive current (viz., b=1) and ion-diffusion controlled one (viz., b=0.5):

$$i(V) = k_1 v + k_2 v^{1/2} \qquad (3)$$

We are interested in the percentage of the capacitive current. So, in order to determine the k_1 value, equation (3) can be reformulated as:

$$i(V) / v^{1/2} = k_1 v^{1/2} + k_2 \qquad (4)$$

Obviously, with a series test of CV curves under different scan speed, the k_1 value can be determined from the linear plots of $i(V)/ \mathrm{v}^{1/2}$ vs $\mathrm{v}^{1/2}$.

In order to obtain the charge per area (which is also a combination of two parts), one can do the following integration.

$$Q = \frac{\int I \bullet dU}{vS} \qquad (5)$$

For example, the capacitance contribution from capacitive behavior is:

$$Q_s = \frac{\int k_1 v dU}{vS} = \frac{k_1}{S} \int dU \qquad (6)$$

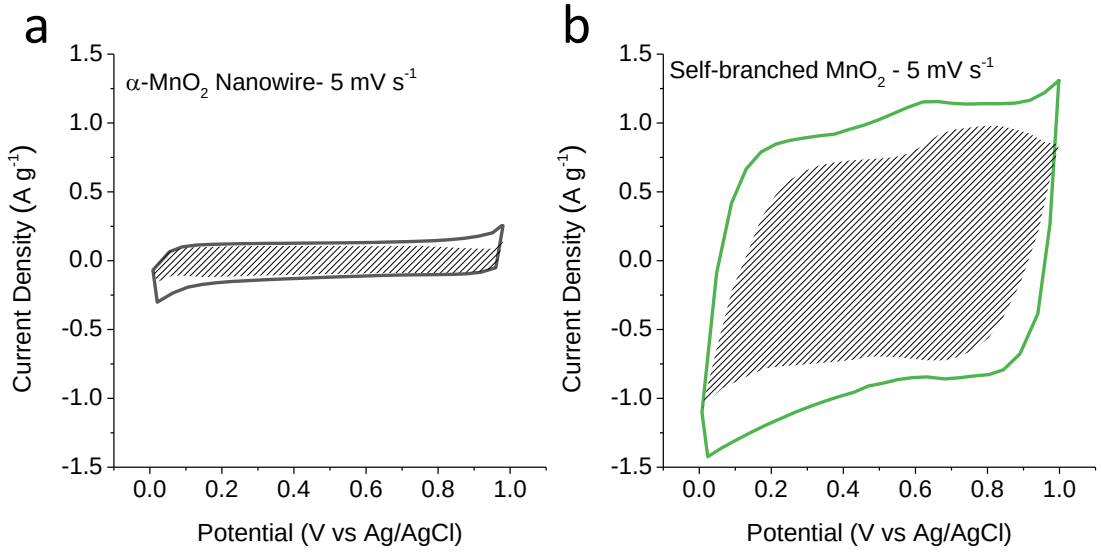

Figure S6. Capacitive contribution calculations of a) α-MnO_2 nanowire and b) self-branched-MnO_2 nanostructure at 5 mV s^{-1}. This figure provides just one example of the current contribution by the capacitive process at this particular sweep rate of 5 mV s^{-1}; For other sweep rates, the pattern differs.

Table S2. Comparison of specific capacitance and areal capacitance at different scan speeds.

Electrode (mass loading in mg/cm²)	Areal capacitance (mF/cm²) @ different scan speed (mV/s)				Gravimetric capacitance (F/g) @ different scan speed (mV/s)			
	1	5	10	20	1	5	10	20
MnO_2-film (0.025)[Brett et al.]	10	-	7.8	6.8	400	-	270	210
Graphene-MnO_2 (3.31)[Xie et al.]	513	430	391	265	155	130	118	80
Graphene-MnO_2 (1.71) [Xie et al.]	325	277	222	197	190	162	130	115
CNT-MnO_2 (1.3) [Cui et al.]	-	189	137	104	-	145	105	80
CNT-MnO_2 (2.1) [Cui et al.]	-	231	189	137	-	110	90	65
CNT-MnO_2 (3.1) [Cui et al.]	-	419	388	233	-	135	125	75
α-MnO_2 (0.5) [Lu et al.]	-	110	107	98	-	220	213	196
Our work (3.37)	783	602	511	392	233	179	152	116

Reference

1. Chen, D.; Ding, D.; Li, X.; Waller, G. H.; Xiong, X.; El-Sayed, M. A.; Liu, M. *Chemistry of Materials* **2015,** 27, (19), 6608-6619.
2. Cheng, S.; Yang, L.; Chen, D.; Ji, X.; Jiang, Z.-j.; Ding, D.; Liu, M. *Nano Energy* **2014,** 9, 161-167.
3. Ede, S. R.; Anantharaj, S.; Nithiyanantham, U.; Kundu, S. *Physical Chemistry Chemical Physics* **2015,** 17, (7), 5474-5484.
4. Julien, C.; Massot, M. *Physical Chemistry Chemical Physics* **2002,** 4, (17), 4226-4235.
5. Julien, C.; Massot, M.; Baddour-Hadjean, R.; Franger, S.; Bach, S.; Pereira-Ramos, J. *Solid State Ionics* **2003,** 159, (3), 345-356.
6. Gao, T.; Glerup, M.; Krumeich, F.; Nesper, R.; Fjellvåg, H.; Norby, P. *The Journal of Physical Chemistry C* **2008,** 112, (34), 13134-13140.
7. Wang, X.; Li, G.; Chen, Z.; Augustyn, V.; Ma, X.; Wang, G.; Dunn, B.; Lu, Y. *Advanced Energy Materials* **2011,** 1, (6), 1089-1093.